Proceedings of ISFOG 2025
5TH INTERNATIONAL SYMPOSIUM ON
FRONTIERS IN OFFSHORE GEOTECHNICS
Nantes, France | June 9-13 2025

ISBN 978-2-85782-758-0

Evaluating the uncertainty in cyclic resistance of sand using a practical cDSS test database

Y. Sun*
Civil Engineering Department, Ghent University, Ghent, Belgium

B. Stuyts, W. Haegeman
Civil Engineering Department, Ghent University, Ghent, Belgium

**yuesun.sun@ugent.be*

ABSTRACT: With the rising demand for offshore wind energy, there is a noticeable trend towards deploying wind turbines with larger blade sizes, positioned farther from coastlines, and facing more complex environmental conditions. A comprehensive understanding of the mechanical properties of marine sediments can facilitate addressing this development trend. The cyclic resistance capacity of soil is typically determined by laboratory tests such as cyclic triaxial (TX) tests and cyclic direct simple shear (DSS) tests. However, due to the inherent variability of soil properties and measurement uncertainties, there is uncertainty on the results of laboratory tests, which has not been thoroughly studied. In this study, results from publicly available data from offshore wind farm projects in Netherlands, are collected and normalized to establish a database. The database comprises various density sediments and different loading conditions, including the basic parameters (e.g., relative density, consolidation stress, over-consolidation ratio) and cyclic properties of the soils (e.g., shear cycle number at specified strain levels). Statistical analysis methods are used to analyse constant volume cyclic DSS testing on marine sands. The database provided three fitting models to obtain cyclic shear stress-number of shear cycles degradation curves, which present reference for further design. In most cases, an increase in average shear stress can enhance the cyclic resistance of the sample, leading to uncertainty. The influence of pre-shear on cyclic resistance varies. Additionally, the correlations between the failure cyclic shear stress ratio at the 10th cycle and the void ratio, effective vertical stress, and over-consolidation are discussed.

Keywords: Cyclic direct simple shear, Database analysis, Constant volume, Sand

1 INTRODUCTION

The construction of offshore wind farms is currently progressing at a faster pace than ever before on a global scale. Before the design and construction of an offshore wind farm, all-side field investigations and laboratory testing are conducted. The capacity of sediments to withstand the cyclic loading from storms and waves is a vital parameter of concern in the long-term behaviour of foundations. To obtain information on cyclic resistance, the cyclic direct simple shear (DSS) test is widely used in related research and industry studies. The cyclic DSS test applies cyclic horizontal shear to sand samples, offering a cost-effective and time-efficient method for determining the cyclic resistance of soil.

Many researchers have conducted extensive studies to investigate the factors affecting cyclic DSS test results and to improve the accuracy of test methods. Control parameters investigated in cyclic DSS tests include cyclic frequency , soil density (Cappellaro et al., 2021), over consolidation ratio , asymmetrical loading (Nong, Park, & Lee, 2021) and pre-shear. Efforts to improve the quality of test results focus on aspects such as confining methods (Baxter, Bradshaw, Ochoa-Lavergne, & Hankour, 2010), preparation methods (Al Tarhouni & Hawlader, 2021), consolidation period (Knut H Andersen, 2015) and control model.

Andersen summarized existing cyclic DSS test data and produced contour diagrams that provide important references for the industry to estimate cyclic resistance based on test results (Knut H. Andersen, 2009; Knut H Andersen, 2015). These empirical diagrams include curves of cyclic shear stress versus number of cycles, namely S-N degradation curve, at failure as well as factors such as asymmetrical loading, relative density, and consolidation stress. From ongoing operations and the construction of offshore wind farms, substantial laboratory test data is accumulated and made publicly available. This data includes traditional tests, such as particle size analysis and oedometer tests, as well as advanced tests like cyclic triaxial and cyclic direct simple shear tests. Such data is valuable for assessing test method performance and understanding marine sediment characteristics. In this study, constant volume cyclic direct simple shear tests from offshore wind farm practices are analysed.

2 DATABASE DESCRIPTION

In this study, a comprehensive database of cyclic direct simple shear (DSS) tests is constructed using publicly available data from offshore wind farm projects in Netherlands (source: https://offshorewind.rvo.nl/). The database comprises approximately 400 cyclic DSS test samples, obtained from six projects. Detailed information of the tests is provided in the associated reports and the Excel files, while some samples are only available in reports. After filtering and selecting based on quality and test conditions, a refined dataset of over 200 constant volume, stress-controlled reconstituted cyclic DSS sand test samples are utilized and analysed. These tests meet standardized procedures in accordance with ASTM D6528-17 and internal company procedures.

The apparatus used for the samples in this database is not equipped with a cell pressure system. All samples use a stack of rings as their lateral confine method, resulting in uncontrolled and unrecorded radial stress. Compared to the reinforced membrane confine method, the rings stack confine method with high lateral stiffness can effectively minimize radial deformation of samples but is associated with relatively high friction. Unlike cyclic triaxial tests, cyclic DSS tests do not require a high degree of saturation, as they lack a cell pressure system necessary to achieve such conditions.

The consolidation stress for different samples is selected based on the in-situ stress levels experienced by the sediment. As a result, samples from upper layers typically undergo lower stress levels compared to those from deeper layers. In certain cases, consolidation stress is applied in multiple stages. The first consolidation stage often involves a higher stress level than the vertical stress at the start of the main cyclic shear stage. Consequently, over-consolidation stress is used for these specimens to reflect their stress history. The over-consolidation ratio (OCR), calculated using Equation (1), is employed to quantify this condition. σ_p' represents the peak historical effective consolidation stress, and σ_v' is the effective vertical stress at start of main cyclic shear stage.

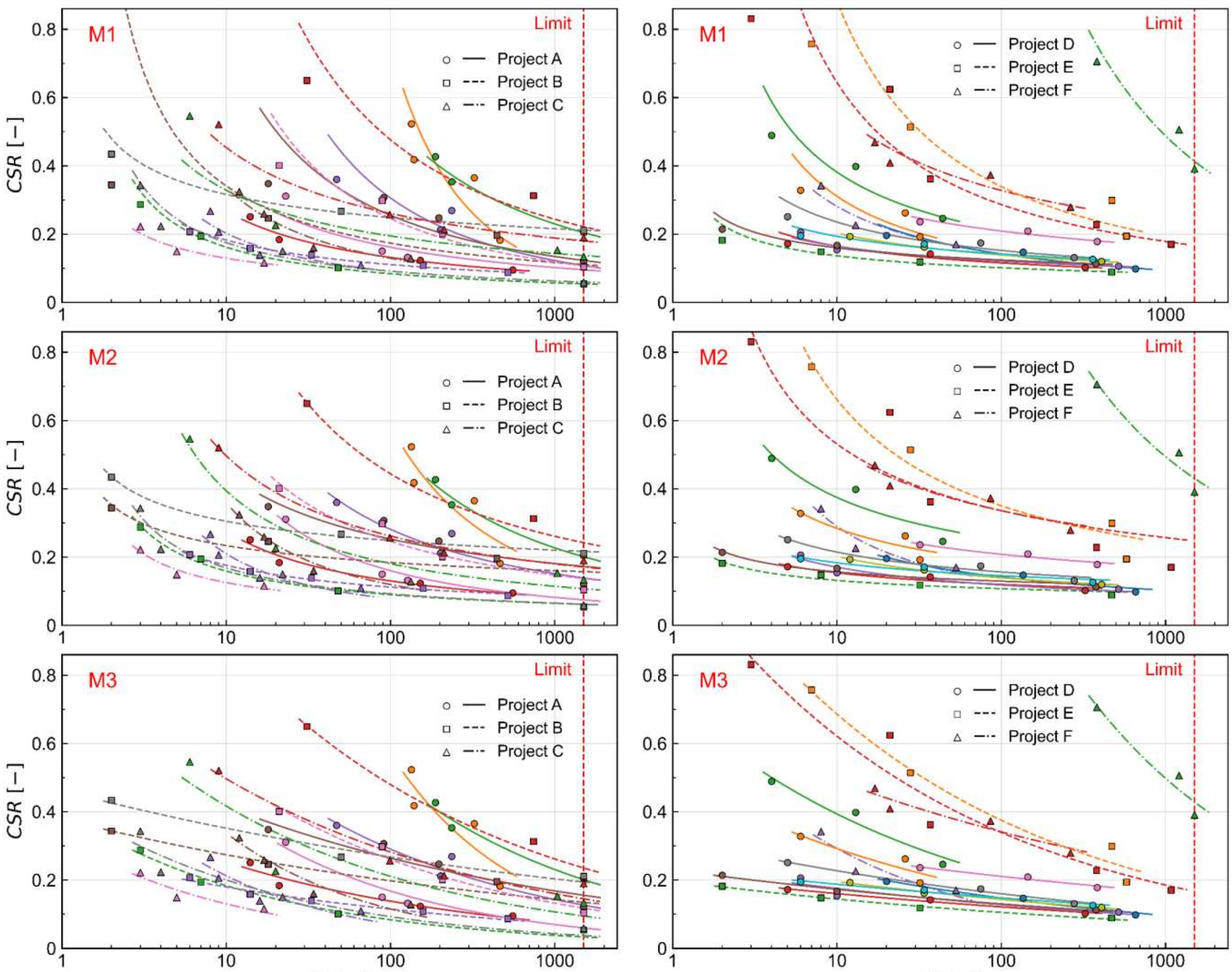

Figure 1 Nf and CSR of Test Points with M1, M2 and M3 S-N Curves

$$OCR = \sigma'_p / \sigma'_v \quad (1)$$

In numerous references (Knut H Andersen, 2015), cyclic and average shear stress are not calculated from effective vertical stress. Instead, a reference vertical stress is used to reduce the influence of consolidation stress, as can be calculated by Equation (2).

$$\sigma'_{ref} = p_a \cdot (\sigma'_v / p_a)^n \quad (2)$$

Here, p_a represent atmosphere pressure (100kPa), and n is an empirical exponent, which is 0.9 for sand and silt. The cyclic shear stress ratio (CSR) and average shear stress ratio (ASR) can then be calculated using Equations (3) and (4). Cyclic shear stress (τ_c) and average shear stress (τ_a) can also be determined when the CSR and ASR are specified.

$$CSR = \tau_c / \sigma'_{ref} \quad (3)$$

$$ASR = \tau_a / \sigma'_{ref} \quad (4)$$

In the test operational procedures, the average shear stress is typically applied as a static shear stress before cyclic shearing. If $\tau_c \leq \tau_a$, some tests are conducted using a one-way shear model.

With the exception for a few specimens designed to study the effects of pre-shear, most specimens are subjected to a pre-shear stage to account for stress history and improve seating between the sand and test apparatus. The pre-shear cyclic stress is set at 5% of the effective vertical consolidation stress, without the application of average stress. After 400 pre-shear cycles under constant vertical stress condition, the specimens are further consolidated to the target vertical stress to facilitate sample drainage.

The cyclic frequency for all samples is 0.1 Hz, which represents a typical wave frequency under storm conditions and is widely accepted in the industry.

The criteria for ending a test generally follow three main rules. The test is terminated when either the average shear strain (γ_a) or the cyclic shear strain (γ_c) reaches 15%. Additionally, if the test reaches 1500 cycles, it is considered complete regardless of whether the shear strain meets the prior conditions. For certain dense samples or under relatively lower CSR conditions, if the maximum cycle limit is reached, a shear strain of 3.75% (either γ_a or γ_c) may be optionally reported in some test documents. Excess pore pressure criteria can also be used to assess the degree of liquefaction. When the maximum excess pore pressure ratio (r_p) exceeds 0.95, the sample is considered to have failed.

3 S-N DEGRADATION CURVES

Cyclic loading can cause particle rearrangement and the generation of excess pore pressure, which explains why cyclic loading can damage a sample at a lower stress level compared to static loading. The relationship between the number of cycles at failure (N_f) and the cyclic shear stress ratio can be depicted in a S-N degradation curve diagram, which provides a reference for understanding the influence of cyclic loading on sand. These S-N degradation curves are essential for estimating the cyclic resistance of sand in design applications. Equation (5) is the most widely used function model and is utilized in the laboratory test reports. In this equation, a and b are the fitting parameters.

$$CSR = a \cdot N_f^b \quad (5)$$

In certain reports, S-N degradation curves are plotted using the best-fit power regression model derived from selected data points and expected trends. These curves are plotted to closely match and replicate Andersen's results, with a greater emphasis on historical database comparisons than on individual test results. However, the detailed plotting method or standard is not disclosed in their reports. Based on the data of the number of cycles at failure, a series of fitting curves are plotted, considering only the best-fit method. Apart from Equation (5), two similar models are also referenced, as shown in Equations (6) and (7).

$$log_{10} N_f = a \cdot CSR^b \quad (6)$$

$$CSR = a \cdot log_{10} N_f^b \quad (7)$$

Equations (6), (7), and (5) are referred to as fitting models M1, M2, and M3, respectively. Figure 1 presents the test points from the database together with the

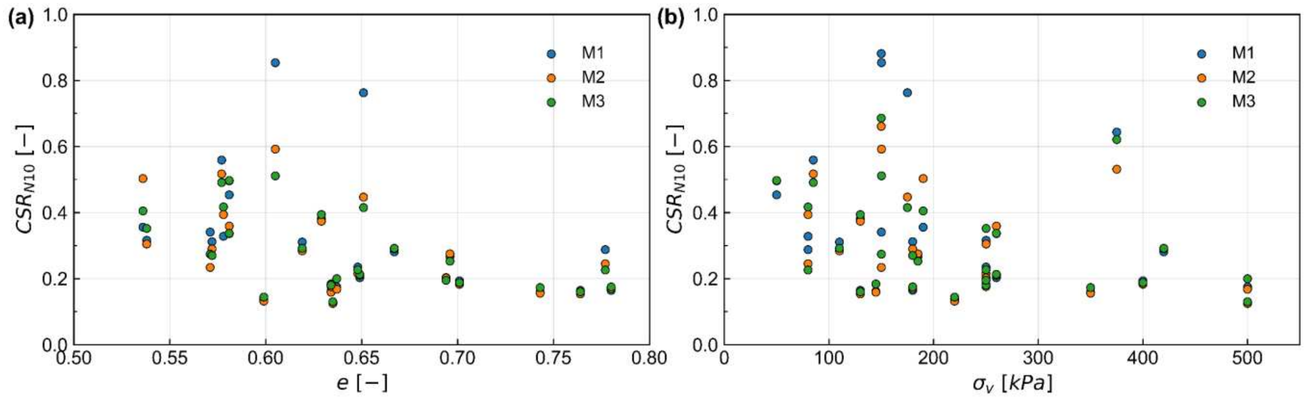

Figure 2 Relationship between CSR_{N10} and e, σ_v

fitted curves. Tests conducted on the same material and under comparable conditions are grouped together. Groups that contain an excessive number of samples with maximum shear cycles (1500), which prevent fitting a curve, or groups with multiple data points that do not exhibit a monotonic trend, are also excluded from these depictions.

A comparison of these three methods reveals that M3 often contributes to significant error in the region of large shear cycles. When compared to Andersen's results, M3 exhibits a similar near-linear pattern for weaker samples but fails to capture the rapid increase observed in relatively dense samples or under high CSR conditions. The M1 model treats CSR as an independent variable and N_f as the dependent variable in tests, demonstrating an ability to minimize the spread in N_f. However, the M1 model generally overestimates the CSR in the region with relatively few cycles. The M2 considers the x-axis on a logarithmic scale. Previous research has shown that the degree of variation tends to increase significantly with the magnitude of shear cyclic number (Sun, Stuyts, & Haegeman, 2024). This model can provide a greater robustness when N_f is large and generates a fitting curve that minimizes the spread in CSR.

$$dx = \frac{\sum_{i=1}^{n}\left|log_{10}\left(\frac{N_f}{f(CSR)}\right)\right|}{n} \quad (8)$$

$$dy = \frac{\sum_{i=1}^{n}\left|CSR - f(N_f)\right|}{n} \quad (9)$$

The average distance between fitting curves and the test points can be calculated using equation (8) and (9), where n is the number of test points; the $f(CSR)$ and $f(N_f)$ denote the fitting results of N_f and CSR respectively. The results obtained are processed by removing outliers that exceeded 1.5 times the interquartile range (IQR). The spread is divided into dx (for N_f) and dy (for CSR), indicating their respective distance in x-axis (log scale) and y-axis. The table 1 presents details on their performance.

Table 1 spread between test points and fitting curves

Model	dx	dx_std	dy	dy_std
M1	0.126	0.062	0.026	0.019
M2	0.191	0.101	0.017	0.011
M3	0.142	0.067	0.311	0.226

The results presented in Table 1 provide numerical evidence supporting the above statements. Each fitting pattern has its own advantages and disadvantages. As noted in some laboratory test reports, applying S-N degradation curves for design purpose should be done in caution.

4 IMPACT OF VARIOUS FACTORS

4.1 Density

Density is one of the most dominant parameters influencing the cyclic resistance of soil. Previous research has shown that as the relative density (D_r) increases (Knut H. Andersen, 2009), larger cyclic shear stress is required to achieve the same number of cycles at failure. The density of the reconstituted samples is determined based on the cone penetration test results, complemented by unit weight, water content, and particle density measurements to closely replicate the natural material conditions. In this study, the laboratory test reports do not indicate the maximum and minimum density of soil samples. However, density information can be obtained and inferred from void ratio (e) and dry density (ρ_d). The sample cyclic resistance is represented by the CSR at $N_f = 10$ (CSR_{N10}) for each group. In the initial analysis step, the linear correlation is conducted for void ratio and other potential parameters, with correlation coefficients provided in Table 2. To prevent single data points from influencing the results, only test groups with a CSR_{N10} of less than 1 are included in the analysis.

The result of correlation coefficient reveals a strong negative linear correlation between void ratio and CSR_{N10} for all three fitting models. To further illustrate the relationship, the test points are plotted in Figure 2 (a). Samples with a low void ratio typically exhibit a higher CSR_{N10}. The distribution of points strongly supports the conclusion that a decreasing void ratio leads to an increase in CSR_{N10}.

Table 2 correlation between CSR_{N10} and e, σ_v and OCR

CSR_{N10}	e	σ'_c	OCR
M1	-0.533	-0.322	0.202
M2	-0.642	-0.381	0.134
M3	-0.705	-0.328	0.201

4.2 Effective vertical stress and OCR

The correlation between consolidation stress and CSR_{N10} is a moderate negative linear correlation, as the values shown in Table 2. Figure 2 (b) provides evidence of this correlation, although it is notably weaker than the correlation with the void ratio. Over-consolidation is generally used to account for historical stress levels that are higher than those at the current positioned layer. In the database, the over-consolidation ratio (OCR) is typically a constant value for each project. More than half of the tests were conducted under $OCR = 1$ condition. Only project D and project E include samples with $OCR > 1$. The database does not have sufficient data points to draw a strong conclusion.

Furthermore, when analyzing the correlation between dx, dy with OCR and σ_c', the results are close to zero indicating no significant linear relationship. This suggests that the uncertainty of test results does not show a linear correlation with OCR and σ_c'.

4.3 Pre-shear

Pre-shear is a standard procedure in conducting cyclic DSS tests. During the pre-shear stage, a significant lower cyclic shear stress is applied on the sample under drained condition. This step accounts for the history of the soil material, including prior dynamic loading events such as earthquakes or long-term wave impacts. Additionally, it improves the seating of the sample within the testing apparatus. Previous research has indicated that pre-shear has a positive effect, as it can enhance the cyclic resistance of the soil. Moreover, when the pre-shear stress increases, the effect of enhancement also increases.

Table 3 shows the test result from the database under identical loading condition and initial stages, except for the presence or absence of a pre-shear stage. The original results are from tests that included pre-shear, while ΔN_f, $\Delta\gamma_a$ and $\Delta\gamma_c$ represent the differences between tests with and without the pre-shear stage. A negative value indicates that the results without pre-shear are lower than those with pre-shear. If ΔN_f is positive, $\Delta\gamma_a$ and $\Delta\gamma_c$ is negative, pre-shear enhances the sample, and vice versa. Among the 16 test groups, 7 groups show an enhancement trend, while 9 groups show a declining trend, indicating that the test database cannot support the conclusion that pre-shear always enhances cyclic resistance. Instead, the data indicates that pre-shear introduces significant variability in its effects on samples.

Table 3 comparison of tests with and without pre-shear

Number	CSR	ΔN_f	$\Delta\gamma_a$	$\Delta\gamma_c$
1	0.122	72	0.74	-0.18
2	0.095	477	1.49	-0.41
3	0.119	0	2.85	0.21
4	0.162	0	-1.88	-1.49
5	0.319	0	1.74	2.74
6	0.166	0	1.48	8.63
7	0.102	241	-0.31	-0.65
8	0.183	0	2.48	-13.26
9	0.182	-1306	-4.02	6.26
10	0.278	0	-0.66	2.16
11	0.101	0	1.09	-0.65
12	0.204	524	-10.9	-1.08
13	0.196	-376	-1.42	0.09
14	0.199	-416	-0.7	0.09
15	0.299	5	-0.7	0.03
16	0.404	0	0.64	-0.02

5 AVERAGE SHEAR STRESS

Unlike clay, the effect of average shear stress on sandy soil is more complex and does not exhibit a monotonic trend. To better illustrate this issue, the test points with an average shear stress ($\tau_a > 0$) from the database are plotted in Figure 3. Due to their different density and test condition, they are grouped using various colors. For clearer understanding of the trend, a series of arrows is drawn to connect pairs of closely related points. The direction of the arrows is determined by N_f, with arrows from bigger numbers to smaller numbers. If two tests have the same number of cycles (e.g., both reaching the limit of 1500 cycles), the permanent shear strain (γ_a) and cyclic shear strain (γ_c) are compared. In such case, the arrows are drawn from points with smaller shear strain toward those with larger shear strain. This method allows the arrows to indicate a transition from a 'safe' test condition to one approaching failure.

By observing the direction of the arrows, the effects of CSR and ASR can be analyzed. The arrows are counted based on their position and direction. For CSR , 84% of the arrows point in the direction of increasing CSR among all arrows showing CSR variation. The remaining 16% that point in the negative direction are also influenced by ASR. This indicates that an increase in CSR generally leads to easier failure.

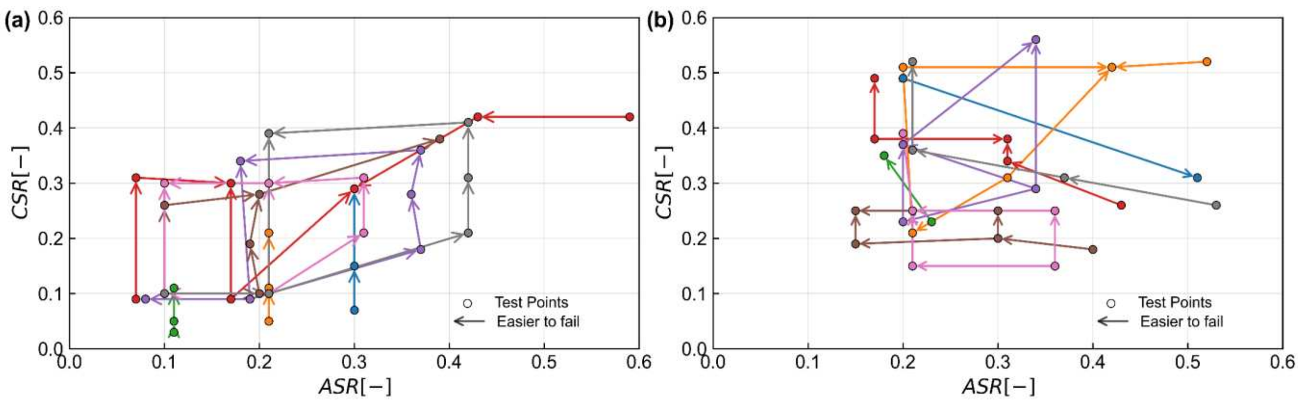

Figure 3 Effect of ASR and CSR

Regarding ASR, 39% of the arrows indicate an increase in ASR, while 61% point in the negative direction among the samples with ASR variation. Additionally, when CSR remains constant, there are 7 arrows pointing in the negative direction compared to only 4 arrows pointing in the positive direction. This leads to the conclusion that the effect of ASR is highly uncertain and increasing average shear stress can enhance the cyclic resistance of samples in most cases. A possible explanation is that average shear stress may cause dense sand samples to exhibit a tendency to dilate under undrained conditions, allowing them to withstand more cycles of shear stress, as noted by Andersen. This characteristic also contributes to the difficulty in establishing a contour diagram for dense sand under asymmetrical loading conditions.

6 CONCLUSION

This study collected several constant volume cyclic direct simple shear (DSS) test results for sandy soil from recent offshore wind farm practices. Based on the analysis of the database, the following conclusions can be summarized.

Three different fitting methods are applied to derive the S-N degradation curves from the test results. The accuracy of these fitting methods is evaluated by calculating the distance between the test results and the fitting curves in two directions.

The influencing factors, including void ratio, effective vertical stress, and over-consolidation ratio, are analyzed. Correlation analysis indicates that the void ratio has a significant linear relationship with CSR_{N10}. The effective vertical stress exhibits a moderate linear relationship, whereas the OCR does not show any linear correlation with the cyclic shear stress ratio. The effect of pre-shear remains uncertain. Based on the current database, no definitive trend regarding the impact of pre-shear can be concluded.

When tests are conducted with an average shear stress, the complexity of the sample's response increases. In most cases, the cyclic stress ratio accelerates the failure of the sample. However, an increase in the average stress ratio does not consistently promote failure. Nonetheless, the trend toward enhanced strength of sample is more significant.

AUTHOR CONTRIBUTION STATEMENT

Y. Sun: Data curation, Formal Analysis, Visualization, Writing- Original draft. **B. Stuyts**: Supervision, Writing- Reviewing and Editing. **W. Haegeman**: Supervision, Writing- Reviewing and Editing

ACKNOWLEDGEMENTS

The authors would like to acknowledge the support of the Belgian Ministry of Economic Affairs through the ETF project WINDSOIL project. The support of VLAIO through the De Blauwe Cluster SBO SOILTWIN project is also acknowledged. The first author is grateful for the financial support provided by the China Scholarship Council.

REFERENCES

Al Tarhouni, M. A., & Hawlader, B. (2021). Monotonic and cyclic behaviour of sand in direct simple shear test conditions considering low stresses. *Soil Dynamics and Earthquake Engineering, 150*, 106931. doi:https://doi.org/10.1016/j.soildyn.2021.106931

Andersen, K. H. (2009). Bearing capacity under cyclic loading — offshore, along the coast, and on land. *Canadian Geotechnical Journal, 46*(5), 513-535. doi:10.1139/t09-003

Andersen, K. H. (2015). Cyclic soil parameters for offshore foundation design. *Frontiers in offshore geotechnics III, 5*, 5-82.

Baxter, C., Bradshaw, A., Ochoa-Lavergne, M., & Hankour, R. (2010). DSS test results using wire-reinforced membranes and stacked rings. In *GeoFlorida 2010: Advances in Analysis, Modeling & Design* (pp. 600-607).

Cappellaro, C., Cubrinovski, M., Bray, J. D., Chiaro, G., Riemer, M. F., & Stringer, M. E. (2021). Liquefaction resistance of Christchurch sandy soils from direct simple shear tests. *Soil Dynamics and Earthquake Engineering, 141*. doi:https://doi.org/10.1016/j.soildyn.2020.106489

Nong, Z.-Z., Park, S.-S., & Lee, D.-E. (2021). Comparison of sand liquefaction in cyclic triaxial and simple shear tests. *Soils and foundations, 61*(4), 1071-1085. doi:10.1016/j.sandf.2021.05.002

Sun, Y., Stuyts, B., & Haegeman, W. (2024). *Statistical Uncertainty of Cyclic Resistance of Sand under Constant Volume Direct Simple Shear.* Paper presented at the 7th International Conference on Geotechnical and Geophysical Site Characterization.